Trade-off between ordinary differential equation and Legendre polynomial methods to study guided modes in angle-ply laminate

Takali, Farid; Nirwal, Sonal; Othmani, Cherif; Groves, Roger M.

DOI
10.1016/j.mtcomm.2022.105208

Publication date
2023

Document Version
Final published version

Published in
Materials Today Communications

Materials Today Communications 34 (2023) 105208

Contents lists available at ScienceDirect

Materials Today Communications

journal homepage: www.elsevier.com/locate/mtcomm

Trade-off between ordinary differential equation and Legendre polynomial methods to study guided modes in angle-ply laminate

Farid Takali [a], Sonal Nirwal [b], Cherif Othmani [c,*], Roger M. Groves [d]

[a] Laboratory of Physics of Materials, Faculty of Sciences of Sfax, University of Sfax, PB 815, 3018 Sfax, Tunisia
[b] Department of Mathematics and Statistics, Manipal University Jaipur, Rajasthan 302034, India
[c] Chair of Acoustics and Haptic Engineering, Dresden University of Technology, 01062 Dresden, Germany
[d] Aerospace NDT Laboratory, Faculty of Aerospace Engineering, Delft University of Technology, Kluyverweg 1, 2629 HS Delft, the Netherlands

ARTICLE INFO

Keywords:
Ordinary differential equation (ODE)
Legendre polynomial
Laminate plates
Coupling properties

ABSTRACT

It has been shown that the roots of guided waves in laminate plates produced by the ordinary differential equations (ODE) approach may not hold under to some computational conditions. A particular drawback of the 2D formulation of the ODE approach is the lack of reliability in the case of unidirectional laminates due to the decoupling properties between the SH and Lamb wave modes, which is caused by the unified matrix of roots. Due to this problem, the SH modes disappear from the unified roots of guided modes, then re-emerge with a separate computation of the SH and Lamb wave modes. Initially, we did not notice this computational "bug" in the event of a coupling between the SH and Lamb wave modes. In this context, the Legendre polynomial method is used to illustrate that fact. Results demonstrate how the polynomial method is pre-eminent to handle the laminate modelling over the ODE method for these specific requirements, however, a trade-off between these two methods needs to be considered to obtain stable and robust behavior of guided dispersion curves. This short study ends with conclusions and future perspectives.

1. Introduction

The advances of composite structures science continues to drive the structural design of aerospace technology such as aircraft and space vehicles. The excellent material properties of multi-layered laminates such as high strength, remarkable design-ability features, and many more capture the attention of industries due to their major role in the development of new advanced structures [1,2]. Some comprehensive assessments on the properties of multi-layered laminates have become available using modeling and numerical approaches. One of these approaches is the Legendre polynomial method, where the problem is converted into an eigenvalue and eigenvector problem [3]. In a recent study, Othmani et al. [4] have employed this polynomial method for computing the effects of elastic constants on guided fundamental modes in homogeneous and sandwich fiber structures. However, when pushed toward modelling the dissimilarities of the multilayer material properties, computations that are reliable require methods that are more accurate. Some comprehensive assessments on this point have become available, such as the work of Yu et al. [5] and the review paper by Othmani et al. [6]. Specifically, Legendre polynomials can deal with laminate plates only when the elastic properties of multilayers do not change significantly [5,6]. Obviously, the higher the numbers of layers, the larger the errors relevant to the polynomial approach [6]. For more extensive background on the polynomial method we recommend reading references [7–12]. The present work is actually motivated by this increased attention to the performance of multi-layered laminates. These shortcomings identified were the main numerical observation, which prompted us to use the ordinary differential equation (ODE) [13]. Dispersion curves obtained from the ODE approach can be used for comparison as this approach is based on an exact analytical treatment for the multilayered structures whatever the dissimilarities of the material properties. Using the ODE approach for a given frequency, the roots of the guided wave modes are calculated by resolving the determinant of the corresponding matrix. Consequently, the search of roots is a critical task, and in this step part of the dispersion curves may be missed. Accordingly, it is important to decrease or remove the relevant errors and suggest strategies to improve the sector of nondestructive testing (NDT), through the trade-off between the ODE and Legendre polynomial methods. It will be very useful to create a well-balanced correlation between high precision roots and reliable results for the

* Corresponding author.
E-mail addresses: othmanicheriffss@gmail.com, cherif.othmani@tu-dresden.de (C. Othmani).

https://doi.org/10.1016/j.mtcomm.2022.105208
Received 16 October 2022; Received in revised form 7 December 2022; Accepted 18 December 2022
Available online 21 December 2022

full ultrasonic frequency range of the system.

The objective of this short communication is to show that the roots of the guided waves produced by the ODE approach may not hold for some computational conditions. Moreover, the ODE approach cannot be used to derive the roots of Lamb and SH modes from the unified matrix in the case of decoupling properties between these both waves, where a separate computational process is still required. However, until recently we did not notice this computational "bug" in calculating the coupling between SH and Lamb modes.

We will use two different structures to illustrate and establish the above-stated assertions. The Legendre polynomial and ODE approaches are first implemented on a unidirectional laminate plate. The elastic properties and the mass density of this composite are highlighted in Reference [4]. Initially, the plate is composed of an 8-ply unidirectional laminate (0°/0°/0°/0°/0°/0°/0°/0°). This example is shown in Fig. 1. Here, the SH and Lamb guided waves can be separately dealt with numerically Γ_{ik}^{SH}&Γ_{ik}^{Lamb}. Here, $\Gamma_{ik}^{SH}$and $\Gamma_{ik}^{Lamb}$are the square matrices. For advantageous numerical operations, particularly on the required computational time, the numerical unified matrix of Lamb and SH modes $\Gamma_{ik}$is strongly recommended. Then, the ODE matrix method is also used to account for the quasi-isotropic laminate (45°/−45°/0°/45°/90°/−45°/0°/90°) as shown in Fig. 2. It has been demonstrated that if there is any misalignment between the material symmetry (for fiber orientation angles that are different to 0° and 90°), guided mode coupling phenomenon is present [14]. Consequently, considering pure Lamb and SH modes as in a traditional symmetric plate is not technically or numerically applicable. Thus, the quasi-isotropic structure breaks the traditional symmetry of a structure, and consequently "true" anti-symmetric and symmetric guided modes no longer exist. Numerically, the unified matrix of guided modes$\Gamma_{ik}$is strongly required at this stage. In this context, the Legendre polynomial method [4,6] is used to illustrate that fact. Results demonstrated how the polynomial method is pre-eminent to handle the problem over the ODE method in the case of unidirectional laminates due to the decoupling properties between the SH and Lamb wave modes.

2. Problem formulation

General unidirectional and quasi-isotropic laminate plates have been depicted schematically in Figs. 1 and 2, respectively. Each layer is characterized by its elastic tensor (C_{ijkl}) and mass density (ρ). These properties have been studied in detail by Othmani et al. [4]. The cartesian coordinates X, Y, and Z are chosen with X in the direction of wave propagation and Z perpendicular to the surface. For such an elastic materials, the dynamic equation is given by,

$$\rho\frac{\partial^2 u_i}{\partial t^2} = \frac{\partial T_{ij}}{\partial x_j} \quad (1)$$

Here, $\rho$is the mass density. $\frac{\partial T_{ij}}{\partial x_j} = C_{ijkl}\frac{\partial^2 u_l}{\partial x_j \partial x_k}$ where (T_{ij}) represents the mechanical stress and (u_l) is the mechanical displacement.

The mechanical displacement in Eq. (1) can be given as follows,

$$u_i = U(x_3) \times \exp\ (\ i\ (k_1 x_1 - \omega\ t)) \quad (2)$$

with, $i = x_1,\ x_2,\ x_3$. ω and k_1 are the angular frequency and wavenumber according $x_1$direction, respectively.

Based on the mechanical stress, the constitutive equation is given by,

$$T_{ij} = C_{ijkl}\frac{\partial u_l}{\partial x_k} \quad (3)$$

However, we can express the derivatives of the mechanical displacement according to the Cartesian coordinate (x_1, x_2, x_3) as,

$$\frac{\partial\ u_1}{\partial x_1} = u_{1,1}, \frac{\partial\ u_2}{\partial x_1} = u_{2,1}, \frac{\partial\ u_3}{\partial x_1} = u_{3,1} \quad (4)$$

$$\frac{\partial\ u_1}{\partial x_3} = u_{1,3}, \frac{\partial\ u_2}{\partial x_3} = u_{2,3}, \frac{\partial\ u_3}{\partial x_3} = u_{3,3} \quad (5)$$

where $\frac{\partial}{\partial x_2} = 0$.

We proceed by putting $j = 1$ in Eq. (3) to get,

$$T_{11} = C_{1111}\ u_{1,1} + C_{1112}\ u_{2,1} + C_{1113}\ u_{3,1} + C_{1131}\ u_{1,3} + C_{1132}\ u_{2,3} + C_{1133}\ u_{3,3} \quad (6)$$

$$T_{21} = C_{2111}\ u_{1,1} + C_{2112}\ u_{2,1} + C_{2113}\ u_{3,1} + C_{2131}\ u_{1,3} + C_{2132}\ u_{2,3} + C_{2133}\ u_{3,3} \quad (7)$$

$$T_{31} = C_{3111}\ u_{1,1} + C_{3112}\ u_{2,1} + C_{3113}\ u_{3,1} + C_{3131}\ u_{1,3} + C_{3132}\ u_{2,3} + C_{3133}\ u_{3,3} \quad (8)$$

and for $j = 3$,

$$T_{13} = C_{1311}\ u_{1,1} + C_{1312}\ u_{2,1} + C_{1313}\ u_{3,1} + C_{1331}\ u_{1,3} + C_{1332}\ u_{2,3} + C_{1333}\ u_{3,3} \quad (9)$$

$$T_{23} = C_{2311}\ u_{1,1} + C_{2312}\ u_{2,1} + C_{2313}\ u_{3,1} + C_{2331}\ u_{1,3} + C_{2332}\ u_{2,3} + C_{2333}\ u_{3,3} \quad (10)$$

$$T_{33} = C_{3311}\ u_{1,1} + C_{3312}\ u_{2,1} + C_{3313}\ u_{3,1} + C_{3331}\ u_{1,3} + C_{3332}\ u_{2,3} + C_{3333}\ u_{3,3} \quad (11)$$

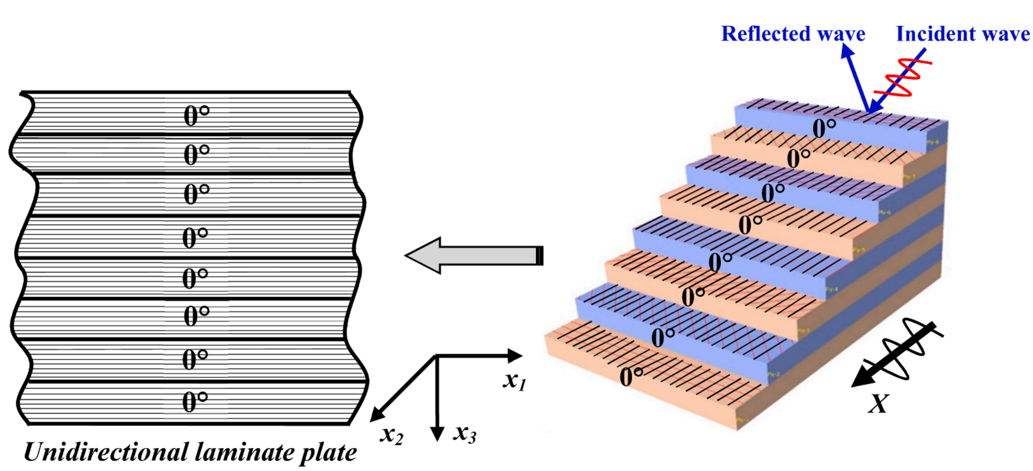

Fig. 1. A schematic configuration of a unidirectional laminate plate 0°/0°/0°/0°/0°/0°/0°/0°. The total thickness of the plate is *H*. The Lamb and SH wave propagation direction is along the x_1.

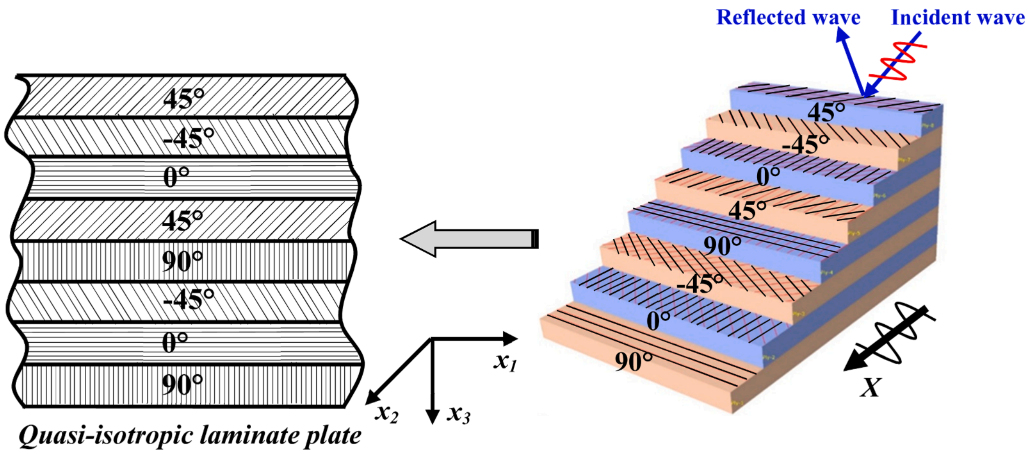

Fig. 2. A schematic configuration of a quasi-isotropic laminate plate 45°/−45°/0°/45°/90°/−45°/0°/90°. The total thickness of the plate is *H*. The Lamb and SH wave propagation direction is along the x_1.

2.1. Ordinary differential equation (ODE)

The ODE procedure employs the so-called "state vector" to determine the eigenvalues and eigenvectors of the total partial waves of the multilayered structures [13],

$$\xi = \begin{bmatrix} U \\ T \end{bmatrix} \tag{12}$$

where, $U = [u_1 \quad u_2 \quad u_3]^T$, $T = [T_{13} \quad T_{23} \quad T_{33}]^T$and we assume that $T' = [T_{11} \quad T_{21} \quad T_{31}]^T$. Eqs. (6)–(11), can be formulated in the form of matrices as [13],

$$\begin{bmatrix} T' \\ T \end{bmatrix} = \begin{bmatrix} \Gamma_{11} & \Gamma_{13} \\ \Gamma_{31} & \Gamma_{33} \end{bmatrix} \begin{bmatrix} U_{,1} \\ U_{,3} \end{bmatrix} \tag{13}$$

where:

$$\Gamma_{ik} = \begin{bmatrix} \Gamma_{11} = \begin{bmatrix} c_{1111} & c_{1121} & c_{1131} \\ c_{2111} & c_{2121} & c_{2131} \\ c_{3111} & c_{3121} & c_{3131} \end{bmatrix} & \Gamma_{13} = \begin{bmatrix} c_{1113} & c_{1123} & c_{1133} \\ c_{2113} & c_{2123} & c_{2133} \\ c_{3113} & c_{3123} & c_{3133} \end{bmatrix} \\ \Gamma_{31} = \begin{bmatrix} c_{1311} & c_{1321} & c_{1331} \\ c_{2311} & c_{2321} & c_{2331} \\ c_{3311} & c_{3321} & c_{3331} \end{bmatrix} & \Gamma_{33} = \begin{bmatrix} c_{1313} & c_{1323} & c_{1333} \\ c_{2313} & c_{2323} & c_{2333} \\ c_{3313} & c_{3323} & c_{3333} \end{bmatrix} \end{bmatrix} \tag{14}$$

Similar to the mechanical displacement$u_i = A\,P_i \exp\,(i\ k_3 x_3) \times \exp(\,i\ (k_1 x_1 - \omega\,t))$, the "state vector" is constructed as [13],

$$\xi = \xi(x_3) \times \exp(\,i\ (k_1 x_1 - \omega\,t)) \tag{15}$$

The mechanical displacements A and P_i denote the unknown functions of $x_3$and polarization, respectively. The equation governing the state of the vector ξ is given by a system of differential equations [13]:

$$\frac{\partial \xi}{\partial\, x_3} = i\, \Re\, \xi \tag{16}$$

Here, $\Re$is the core equation used in the ODE method, which is the so-called "Acoustic Fundamental Tensor". It is worth noting that the $\Re$ is based on six partial waves, which specifically lead to three downward waves and three upward waves.

At this stage, let us develop the second line of Eq. (13), with$\frac{\partial}{\partial x_1} = i\, k_1$, to get this system [13]:

$$\frac{\partial U}{\partial x_3} = i\ \left[-k_1\, \Gamma_{33}^{-1}\, \Gamma_{31}, -i\, \Gamma_{33}^{-1} \right]\ \xi \tag{17}$$

By substituting the mechanical displacement $u_i = A\,P_i \exp\ (i\ k_3 x_3) \times \exp(\ i\ (k_1 x_1 - \omega\, t))$ into Eq. (1), the following three equations can be obtained:

$$\begin{cases} \dfrac{\partial T_{13}}{\partial x_3} = -\rho\, \omega^2 u_1 - \dfrac{\partial T_{11}}{\partial x_1} \\ \dfrac{\partial T_{23}}{\partial x_3} = -\rho\, \omega^2 u_2 - \dfrac{\partial T_{21}}{\partial x_1} \\ \dfrac{\partial T_{33}}{\partial x_3} = -\rho\, \omega^2 u_3 - \dfrac{\partial T_{31}}{\partial x_1} \end{cases} \tag{18}$$

where$\frac{\partial^2 u_i}{\partial t^2} = -\omega^2 u_i$. Eq. (18) can be contracted using the two vectors (T) and (T') (Eq. (13)) and the mechanical displacement (U) (Eq. (12)) as follows [13]:

$$\frac{\partial T}{\partial x_3} = -\rho\, \omega^2 I'\ U - \frac{\partial T'}{\partial x_1} \tag{19}$$

where $I' = \begin{bmatrix} 1 & 0 & 0 \\ 0 & 1 & 0 \\ 0 & 0 & 1 \end{bmatrix}$.

By substituting the second line of Eq. (13) and Eq. (17) into Eq. (19) the following equation is obtained [13]:

$$\frac{\partial T}{\partial x_3} = i\ \left[-i\left(\Gamma_{11} - \Gamma_{13}\Gamma_{33}^{-1}\Gamma_{31}\right) k_1^2 + i\,\rho\,\omega^2\, I',\ -i\, k_1\, \Gamma_{13}\, \Gamma_{33}^{-1} \right]\ \xi \tag{20}$$

By grouping Eqs. (19) and (20), the "Acoustic Fundamental Tensor" is found as [13]:

$$\Re = \begin{bmatrix} -k_x \Gamma_{33}^{-1} \Gamma_{31} & -i\Gamma_{33}^{-1} \\ -i\left(\Gamma_{11} - \Gamma_{13}\Gamma_{33}^{-1}\Gamma_{31}\right) k_x^2 + i\rho\omega^2 I' & -k_x \Gamma_{13} \Gamma_{33}^{-1} \end{bmatrix} \tag{21}$$

By considering the characteristics of laminate plates (Figs. 1 and 2), the size of involved matrices in Eq. (21) is reduced significantly, where the unidirectional and quasi-isotropic laminates are considered. Barski and Pajak et al. [15] have pointed out that the search of dispersion curves using the majority of matrix methods may be a boring task, and some of the roots may be missed. Thus, the question remains open concerning the ODE numerical procedure. ***"Will this matrix approach be capable of handling the two unidirectional and quasi-isotropic laminates with the same potential"?*** Eq. (13) shows that the Lamb and SH wave modes coupling phenomena can potentially be adjustabed byΓ_{ik}, instead of using the "Acoustic Fundamental Tensor"$\Re(6 \times 6)$.

In the present work, the decoupled symmetric and anti-symmetric families of the SH and Lamb wave modes exist only for the unidirectional laminates. Thereby, the characteristics of Lamb modes can be controlled with this separate matrix:

$$\Gamma_{ik}^{Lamb} = \begin{bmatrix} C_{1i1k} & C_{1i3k} \\ C_{3i1k} & C_{3i3k} \end{bmatrix} \quad (22)$$

Here, the size of "Acoustic Fundamental Tensor" becomes$\Re(4\times4)$ and the state of the vector $\xi = [u_1 \quad u_3 \quad T_{13} \quad T_{33}]^T$.

A similar geometry of the SH wave modes could be stated as follow:

$$\Gamma_{ik}^{SH} = [C_{2i2k}] \quad (23)$$

where $\Re(2\times2)$ and $\xi = [u_2 \quad T_{23}]^T$. Eqs. (22) and (23) presents the matrix inversion as the core critical limitation of the ODE method used in the present work.

2.2. Legendre polynomial

The work of Othmani et al. [4] gives a detailed observation on the Legendre polynomial method to compute the guided dispersion curves in composites. As mentioned before, the Legendre polynomial approach [4,6] is based on the polynomial approximation basis which automatically incorporates the different boundary conditions by introducing the rectangular window function $\pi_{0,kh}(x_3)$[4,6]: $\pi_{0,kh}(x_3) = \begin{cases} 1, 0 \le x_3 \le kH \\ 0 otherwise \end{cases}$.

This subsection is dedicated to the remind snapshot of the fundamental aspects of how guided roots can be computed using the polynomial approach.

Substituting Eq. (2) and Eqs. (6)–(11) into Eq. (1) yields,

$$-\rho\times\left(\frac{\omega^2}{k^2}\right)\times U_1 = -(C_{11}\times U_1) + (i\times(C_{13}+C_{55})\times U_3{}') + (C_{55}\times U_1{}'') \\ +(i\times C_{55}\times U_3\times(\delta(q_3=-1)-\delta(q_3=1))) + (C_{55}\times U_1{}'\times(\delta(q_3=-1)-\delta(q_3=1))) \quad (24a)$$

$$-\rho\times\left(\frac{\omega^2}{k^2}\right)\times U_2 = -(C_{66}\times U_2) + (C_{44}\times U_2{}'') + (C_{44}\times U_2{}'\times(\delta(q_3 \\ =-1)-\delta(q_3=1))) \quad (24b)$$

$$-\rho\times\left(\frac{\omega^2}{k^2}\right)\times U_3 = -(C_{55}\times U_3) + (i\times(C_{31}+C_{55})\times U_1{}') + (C_{33}\times U_3{}'') \\ +(i\times C_{31}\times U_1(\delta(q_3=-1)-\delta(q_3=1))) + (C_{33}\times U_3{}'\times(\delta(q_3=-1)-\delta(q_3=1))) \quad (24c)$$

where (') denotes the partial derivative with respect toq_3. However, the Cartesian coordinates (x_1, x_3) have been transformed to a dimensionless form $q_1 = k\,x_1$and $q_3 = k\,x_3$. The Kronecker delta function $\delta(x-x_0)$ is defined$\frac{\partial\pi_{0,kH}}{\partial q_3} = [\delta(0) - \delta(q_3 - kH)]$.

Obviously, Eq. (24b) is independent of Eqs. (24a) and (24c). Actually, Eq. (24b) controls the propagating of SH modes, while Eqs. (24a) and (24c) represent the propagation of Lamb modes.

The unknown $U_i(q_3)$is given in terms of a polynomial approximation as follows [4,6]:

$$U_i(q_3) = \sum_{m=0}^{\infty} p_m^i \sqrt{\frac{2m+1}{kH}} P_m\left(\frac{2q_3}{kH}-1\right) \quad , \ i = 1,\ 2,\ 3 \quad (25)$$

where p_m^i is the expansion coefficient andP_m is Legendre polynomials of order$m$.

Substituting Eq. (25) into Eq. (24), multiplying by $\sqrt{\frac{2j+1}{kH}} P_j^*\left(\frac{2q_3}{kH}-1\right)$ and integrating over $q_3$from (0) to (kH)gives

$$(\Omega^2\times p_m^1) = -M_{jm}^{-1}\left[\aleph_{11}^{jm} p_m^1 + \aleph_{13}^{jm} p_m^3\right] \quad (26a)$$

$$(\Omega^2\times p_m^2) = -M_{jm}^{-1}\left[\aleph_{22}^{jm} p_m^2\right] \quad (26b)$$

$$(\Omega^2\times p_m^3) = -M_{jm}^{-1}\left[\aleph_{31}^{jm} p_m^1 + \aleph_{33}^{jm} p_m^3\right] \quad (26c)$$

where $\Omega = \left(\frac{\omega}{k}\right)$. Then, the above block matrices can easily be solved in the form of eigenvalue and eigenvector problem using the Matlab command "eig". Moreover, it is worth noting that the same numerical procedure of polynomial method is found for the quasi-isotropic laminate (case of coupling between SH and Lamb wave modes).

3. Analysis of results

In this section, our aim is to assess the efficiency of the ODE approach with both the coupling and decoupling properties of guided modes. A computer program was formulated in Matlab to calculate the dispersion curves. Initially, the SH and Lamb guided waves in 0°/0°/0°/0°/0°/0°/0°/0° unidirectional laminate were separately dealt with. Here, the purely Lamb and SH modes are applicable. However, the presence of a unified matrix of Lamb and SH waves can also be considered as a possible solution of the guided dispersion curves since this is not considered to prejudice the symmetry of the plate. Firstly, we will discuss some results that have been computed for predicting dispersion curves using the unified matrix Γ_{ik}(Eq. (14)). Accordingly, Fig. 3 shows the Lamb and SH dispersion curves in the 0°/0°/0°/0°/0°/0°/0°/0° unidirectional laminate plate using ODE and Legendre polynomial (truncation order M = 15) methods. Here, we can observe both the lamb (symmetric and anti-symmetric) and SH modes.$S_n(n = 0, 1,.,4)$, $A_n(n = 0, 1,.,4)$and $SH_n(n = 0, 1,.,9)$ represent the symmetric Lamb modes, the anti-symmetric Lamb modes, and shear horizontal modes. In contrast to common expectations, we observe a new observation using the ODE approach: a lack of SH modes and the appearance of Lamb modes only. However, before writing down some relevant notifications, the ODE method was extended to take into account the SH and Lamb modes, separately. Thus, the both square matrices Γ_{ik}^{SH}(Eq. (23)) and Γ_{ik}^{Lamb} (Eq. (22)) are considered. It is noted that the major drawback of

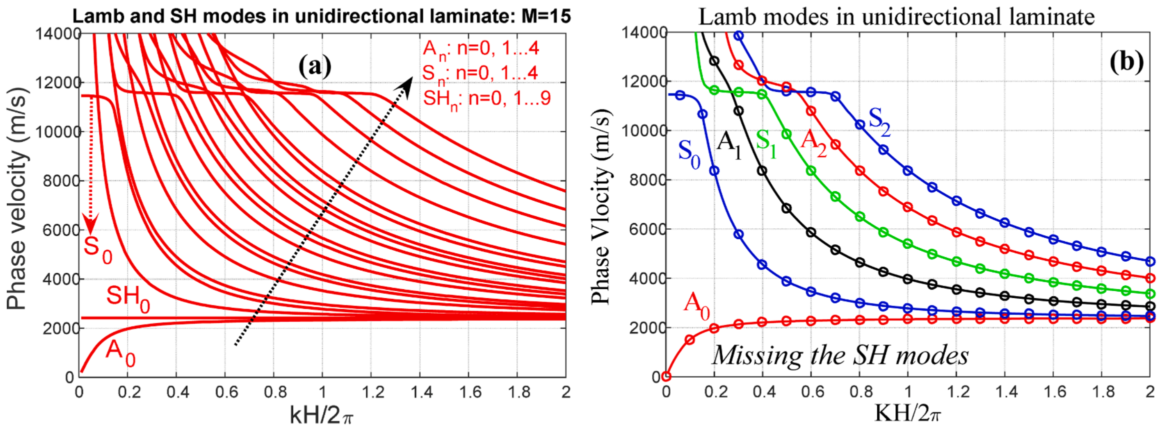

Fig. 3. SH and Lamb modes in the unidirectional laminate plate 0°/0°/0°/0°/0°/0°/0°/0° (a) the Legendre polynomial method and (b) the ODE method with Eq. (14).

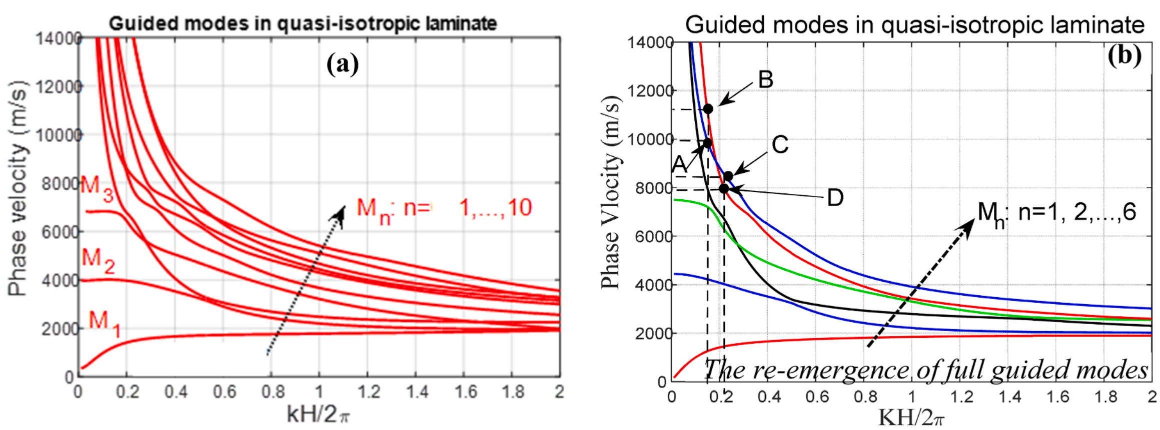

Fig. 4. Guided modes in the quasi-isotropic laminate plate 45°/−45°/0°/45°/90°/−45°/0°/90° determined using (a) the Legendre polynomial method and (b) the ODE method with Eq. (14).

this separate strategy is that they are very time-consuming (two separate codes) and is a monotonous task. Numerical results demonstrate that the SH modes re-emergence with this separate computational of SH and Lamb modes, however they are not included here for brevity. Therefore, this numerical “bug” is closely related to the dominance of the Lamb modes compared to the SH wave modes. In addition, another possible cause for this "bug" is the presence of 2D plane-strain problem, which may result in "disappearing" of SH-modes for materials with certain classes of symmetry. It is noted that the roots of the guided waves using Legendre polynomial approach are retrieved with an acceptable discrepancy [6]. This discrepancy is attributed to the use of the contrast of adjacent layers [6]. From the physics point of view, it can be observed that the phase velocity of $A_0$is dispersive in the lower range of $kh/2\pi$, however for $kh/2\pi > 0.6$, the curve displays a static motion over the entire range. On the other hand, the curve exhibits a decreasing behavior for $kh/2\pi < 1$, while the curve shows a stationary mode. However, the SH_0 mode showed a constant behavior for the entire range of $kh/2\pi$. At this stage, the question becomes “***will matters ever be the same for the 45°/−45°/0°/45°/90°/−45°/0°/90° quasi-isotropic laminate again?*** “. As mentioned above, this structure breaks the conventional symmetry of a laminate plate, and consequently "true" anti-symmetric and symmetric guided modes no longer exist, while guided modes still propagate in the plate. Let us denote the guided modes as M_0, M_1, M_2,. M_n. Thus, the guided mode dispersion curves in this quasi-isotropic laminate answers this need and sets forth the exploration of the numerical state. Data reported in Fig. 4 clearly show that the guided dispersion curves obtained by the ODE approach are consistent with the classical observation calculated by the polynomial method (truncation order M = 20). Thereby, we did not notice any ODE computational "bug" in the event of a coupling between the SH and Lamb modes (quasi-isotropic laminate).

The present polynomial and ODE methods cannot separate the computation of the phase velocity of each modes. Thereby, the crossings amongst modes remains suspect (Fig. 4). A more general validation method based on the mechanical displacements answers this need and sets forth to explore how true is the intertwining between modes (Fig. 4). For a more extensive background on this strategy, we recommend reading Reference [16]. Here, the labelled points A, B, C and D in Fig. 4 are considered, while the ODE method is used to calculate the mode profiles. The "symmetry" of the displacement shapes of relevant modes is computed and illustrated before and after the suspected intersection (e. g. A-C and B-D). Fig. 5 shows the mode profiles of the mechanical displacements in the 45°/−45°/0°/45°/90°/−45°/0°/90° quasi-isotropic laminate plate at the points, which are labelled as A, B, C and D in Fig. 4. The mode shapes for M_5 in Fig. 5(a) and (c) corresponding to the labelled points A (before the suspected crossing) and C (after the suspected crossing) are both quasi-symmetric. Instead, the mode shapes for the labelled points B and D (mode M_6) are both quasi-antisymmetric. This observation confirms that there must indeed be an intertwining between the M_5 and M_6 points and not only an approaching of both curves with a subsequent separation.

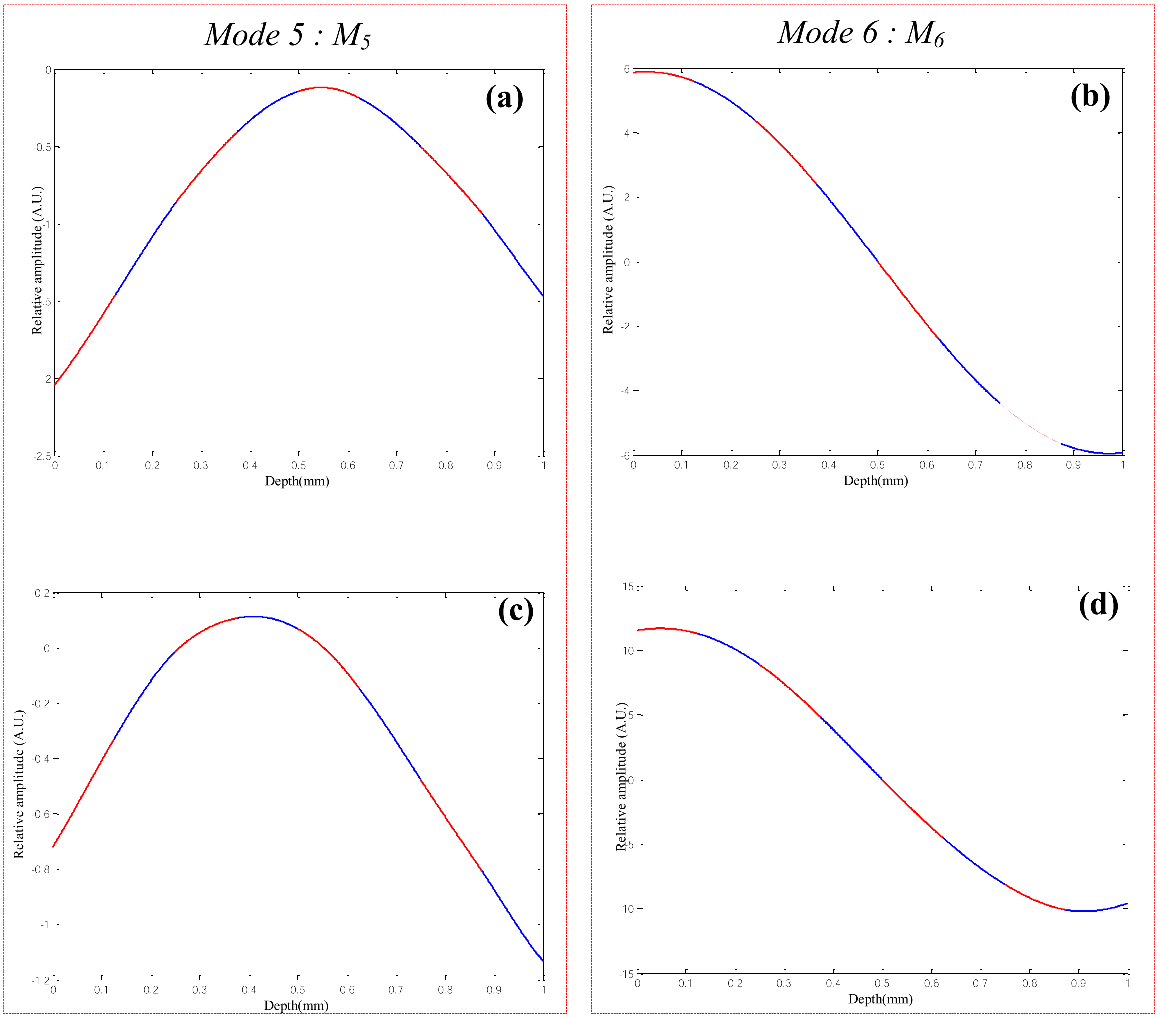

Fig. 5. Mechanical displacements of guided modes in the unidirectional laminate plate 45°/−45°/0°/45°/90°/−45°/0°/90°: (a), for the point labeled A (kH/2π = 0.15, V_{ph} = 9941.6 m/s); (b), for the point labeled B (kH/2π = 0.15, V_{ph} = 1184 m/s); (c), for the point labeled C (kH/2π = 0.22, V_{ph} = 8535.4 m/s); (d), for the point labeled D (kH/2π = 0.22, V_{ph} = 7980.5 m/s).

4. Conclusions

The ordinary differential equations (ODE) approach can be used for finding the exact roots of guided waves in laminates with the help of Matlab computation. Unfortunately, there is a critical condition when a straightforward and formal application of the ODE approach has produced incomplete results. Accordingly, we observed a new surprising observation: a lack of SH modes and only the appearance of Lamb modes in the unidirectional laminates. Therefore, under this structure condition the use of the separate strategy is strongly recommended. Instead, this computational "bug" did not happen in the event of a coupling between SH and Lamb modes. It can be noted that a polynomial alternative approach for finding full roots in unidirectional laminates exists, but only when the two adjacent layers' properties do not change significantly. Thus, it has been demonstrated that this polynomial expansion can be successfully and efficiently used for solving guided roots under this condition. It is therefore worth noting that there is a trade-off between the ODE and Legendre polynomial methods. In the case of decoupling properties between SH and Lamb waves, useful results using a polynomial approach can be achieved. However, this approach leads to slight errors in phase velocities, which can increase when increasing the number of layers numbers. In this condition, the ODE approach is strongly recommended. Instead, when there are coupling properties between SH and Lamb modes, the lack of reliability of the ODE method is obvious, and then the Legendre polynomial approach is strongly recommended. Thus, it is interesting to consider these drawbacks in a trade-off.

For numerical methods to study guided dispersion curves in composite laminate, great achievements have been made regarding the accurate relevant roots, as mentioned in this work. However, for better development and utilization of these numerical methods, there are still some challenges to consider. One of them is an accurate solution for the guided modes in the unidirectional laminates with dissimilar properties with a large number of layers [17–19]. Nevertheless, neither the polynomial approach nor the ODE method can give a reliable roots pattern under this condition. Hence, an improved version of the Legendre polynomial method will be needed to obtain stable and reliable roots in the future. In addition, since the ODE "bug" is surprising, a possible way to gain further understanding might be following the complete 3D formulation of the ODE-like approach [20].

Declaration of Competing Interest

The authors declare that they have no known competing financial interests or personal relationships that could have appeared to influence the work reported in this paper.

Data Availability

No data was used for the research described in the article.

Acknowledgments

The author ***Farid TAKALI*** acknowledges the financial support of Tunisian Ministry of Higher Education, Scientific Research (LPM laboratory).

References

[1] S. Guha, A.K. Singh, Plane wave reflection/transmission in imperfectly bonded initially stressed rotating piezothermoelastic fiber-reinforced composite half-spaces, Eur. J. Mech. A Solids 88 (2021), 104242.
[2] A.K. Singh, P. Rajput, S. Guha, S. Singh, Propagation characteristics of love-type wave at the electro-mechanical imperfect interface of a piezoelectric fiber-reinforced composite layer overlying a piezoelectric half-space, Eur. J. Mech. A Solids 93 (2022), 104527.
[3] J.G. Yu, J.E. Lefebvre, Ch Zhang, Guided wave in multilayered piezoelectric–piezomagnetic bars with rectangular cross-sections, Compos. Struct. 116 (2014) 336–345.
[4] C. Othmani, A. Njeh, M.H. Ben Ghozlen, Influences of anisotropic fiber-reinforced composite media properties on fundamental guided wave mode behavior: a legendre polynomial approach, Aerosp. Sci. Technol. 78 (2018) 377–386.
[5] J.G. Yu, J.E. Lefebvre, Y.Q. Guo, Free-ultrasonic waves in multilayered piezoelectric plates: An improvement of the Legendre polynomial approach for multilayered structures with very dissimilar materials, Compos.: Part B 51 (2013) 260–269.
[6] C. Othmani, H. Zhang, C.F. Lu, Y.Q. Wang, A.R. Kamali, Orthogonal polynomial methods for modeling elastodynamic wave propagation in elastic, piezoelectric and magneto-electro-elastic composites—a review, Compos. Struct. 286 (2022), 115245.
[7] J.G. Yu, X. Wang, X. Zhang, Z. Li, F. Li, An analytical integration Legendre polynomial series approach for Lamb waves in fractional order thermoelastic multilayered plates, Math. Methods Appl. Sci. 45 (2022) 7631–7651.
[8] X. Zhang, Z. Li, X. Wang, J.G. Yu, The fractional Kelvin-Voigt model for circumferential guided waves in a viscoelastic FGM hollow cylinder, Appl. Math. Model. 89 (2021) 299–313.
[9] M. Zheng, H. Ma, Y. Lyu, C. Lu, C. He, Derivation of circumferential guided waves equations for a multilayered laminate composite hollow cylinder by state-vector and Legendre polynomial hybrid formalism, Compos. Struct. 255 (2021), 112950.
[10] M. Zheng, C. He, Y. Lu, B. Wu, State-vector formalism and the Legendre polynomial solution for modelling guided waves in anisotropic plates, J. Sound Vib. 412 (2018) 372–388.
[11] M. Zheng, H. Ma, Y. Lyu, C. He, C. Lu, On the dispersion of cylinder guided waves propagating in a multilayer composite hollow cylinder made of anisotropic materials, Aerosp. Sci. Technol. 95 (2019), 105432.
[12] J. Gao, Y. Lyu, M. Zheng, M. Liu, H. Liu, H. Liu, B. Wu, C. He, Modeling guided wave propagation in multi-layered anisotropic composite laminates by state-vector formalism and the Legendre polynomials, Compos. Struct. 228 (2019), 111319.
[13] F. Takali, C. Othmani, C.F. Lu, Influence of gold electrode layers on the SH waves propagation in sandwich structures based on Au/PMN-0.33PT/Au and Au/PZT-5H/Au: Numerical implementation, Mater. Sci. Eng. B 272 (2021), 115383.
[14] C. He, H. Liu, Z. Liu, B. Wu, The propagation of coupled Lamb waves in multilayered arbitrary anisotropic composite laminates, J. Sound Vib. 332 (2013) 7243–7256.
[15] M. Barski, P. Pajak, Determination of dispersion curves for composite materials with the use of stiffness matrix method, Acta Mech. et Autom. 11 (2017) 121–128.
[16] C. Othmani, H. Zhang, A.R. Kamali, C.F. Lü, F. Takali, B. Köhler, Propagating, evanescent and ZGV Lamb modes in high-performance anisotropic Cu–Al–Ni alloy plates, Arch. Appl. Mech. 92 (2022) 21–43.
[17] Y. Sun, Y. Zhang, H. Long, Y. Sun, L. Zou, X. Yang, Friction stir lap welding for dissimilar materials of aluminum alloy and carbon-fiber-reinforced polyetherimide, Mater. Today Commun. 33 (2022), 104427.
[18] A. Amanollahi, I. Ebrahimzadeh, M. Raeissi, N. Saeidi, Laminated steel/aluminum composites: Improvement of mechanical properties by annealing treatment, Mater. Today Commun. 29 (2021), 102866.
[19] Y.D. Boon, S.C. Joshi, A review of methods for improving interlaminar interfaces and fracture toughness of laminated composites, Mater. Today Commun. 22 (2020), 100830.
[20] A.K. Mal, Wave propagation in layered composite laminates under periodic surface loads, Wave Motion 10 (1988) 257–266.